NUCL SCI TECH (2021) 32:103
https://doi.org/10.1007/s41365-021-00946-3

Systematics on production of superheavy nuclei $Z = 119 - 122$ in fusion-evaporation reactions

Fei Niu[1] · Peng-Hui Chen[2] · Zhao-Qing Feng[1]

Received: 1 July 2021 / Revised: 26 August 2021 / Accepted: 29 August 2021 / Published online: 29 September 2021

Abstract The fusion dynamics of the formation of superheavy nuclei were investigated thoroughly within the dinuclear system model. The Monte Carlo approach was implemented in the nucleon transfer process to include all possible orientations, at which the dinuclear system is assumed to be formed at the touching configuration of dinuclear fragments. The production cross sections of superheavy nuclei Cn, Fl, Lv, Ts, and Og were calculated and compared with the available data from Dubna. The evaporation residue excitation functions in the channels of pure neutrons and charged particles were systematically analyzed. The combinations of ^{44}Sc, ^{48,50}Ti, ^{49,51}V, ^{52,54}Cr, ^{58,62}Fe, and ^{62,64}Ni bombarding the actinide nuclides ^{238}U, ^{244}Pu, ^{248}Cm, ^{247,249}Bk, ^{249,251}Cf, ^{252}Es, and ^{243}Am were calculated to produce the superheavy elements with $Z = 119 - 122$. We obtained that the production cross sections sensitively depend on the neutron richness of the reaction system. The structure of the evaporation residue excitation function is related to the neutron separation energy and fission barrier of the compound nucleus.

Keywords Dinuclear system model · Fusion-evaporation reactions · Superheavy nuclei · Cross sections

This work was supported by the National Natural Science Foundation of China (Nos. 12175072 and 11722546) and the Talent Program of South China University of Technology.

✉ Zhao-Qing Feng
fengzhq@scut.edu.cn

[1] School of Physics and Optoelectronic Technology, South China University of Technology, Guangzhou 510640, China

[2] College of Electrical Energy and Power Engineering, Yangzhou University, Yangzhou 225000, China

1 Introduction

Over the past decades, the synthesis of superheavy nuclei (SHN) has attracted much attention. SHN synthesis has been achieved in experiments via massive fusion reactions. The seventh period in the periodic table was filled with the superheavy element tennessine (Ts) using the Dubna gas-filled recoil separator (DGFRS) at the Flerov Laboratory of Nuclear Reactions in Dubna, Russia [1]. The existence of superheavy elements (SHE) was predicted in the late 1960s by the macroscopic-microscopic theory of the atomic nucleus [2]. The synthesis of SHN is associated with testing the shell model beyond the doubly magic nucleus ^{208}Pb, searching for the "island of stability," exploring the limit of the mass of atomic nucleus, and providing a strong Coulomb field such as quantum electrodynamics (QED) in a super-strong electric field [3]. The superheavy nucleus (SHN) ($Z \geq 106$) exists due to the strong binding shell effect against Coulomb repulsion. Therefore, the position of shell closure is particularly significant for the properties of SHN, such as half-lives of the α decay chain and spontaneous fission, formation probability, etc.; theoretical models predicted the shell closures at $Z = 114$ and $N = 184$ [4, 5]. Attempts to synthesize elements beyond Og ($Z = 118$) were performed using different systems, for example, ^{64}Ni+^{238}U [6], ^{58}Fe+^{244}Pu [7], ^{54}Cr+^{248}Cm [8, 9], and ^{50}Ti+^{249}Cf [10]. The mass and angle distributions of fission fragments were measured [11]. Systematic analysis of different reactions are required for preferentially producing new SHNs in experiments.

The history of the synthesis of SHN goes back 40 years when multi-nucleon transfer reactions in collisions of two actinide nuclei were conducted [12, 13]. However, the

yields of the heavy fragments in strongly damped collisions were found to decrease rapidly with increasing atomic numbers and were unable to produce SHN because of the significantly low cross section. Combinations with a doubly magic nucleus or nearly magic nucleus are usually chosen owing to the larger reaction Q values. Reactions with ^{208}Pb or ^{209} Bi-based targets were first proposed by Oganessian et al. [14, 15]. The SHEs from Bh to Cn were synthesized in the cold fusion reactions at GSI (Darmstadt, Germany) with the heavy-ion accelerator UNILAC and the SHIP separator [16, 17]. Experiments on the synthesis of element Nh ($Z = 113$) in the ^{70}Zn+^{209}Bi reaction were performed successfully at RIKEN (Tokyo, Japan) [18]. However, creating superheavy isotopes beyond Nh in cold fusion reactions is challenging because of the significantly low cross section ($\sigma < 0.1$ pb). Superheavy elements from Fl ($Z = 114$) to Og ($Z = 118$) were synthesized at the Flerov Laboratory of Nuclear Reactions (FLNR) in Dubna (Russia) with the double magic nuclide ^{48}Ca bombarding actinide nuclei [19–22]; in this experiment, more neutron-rich SHN was produced and identified by the subsequent α-decay chain. The decay properties of ^{271}Ds in the cold fusion reaction of ^{64}Ni+^{208}Pb$\rightarrow$^{271}Ds+n were identified using a gas-filled recoil separator at the Institute of Modern Physics (IMP) in Lanzhou [23]. Constructing new facilities worldwide, such as RIBF (RIKEN, Japan), SPIRAL2 (GANIL in Caen, France), FRIB (MSU, USA), and HIAF (IMP, China), and using significantly neutron-rich radioactive beams, we can potentially create SHNs on the "island of stability" soon.

The formation dynamics of SHN in massive fusion and multinucleon transfer reactions are complicated, and are associated with the coupling of several degrees of freedom, such as radial elongation, mass or charge asymmetry, shape configuration, relative motion energy, etc. Several macroscopic models were developed to describe the fusion hindrance in massive systems, for example, the macroscopic dynamical model [24], fusion-by-diffusion (FBD) model [25, 26], dynamical models based on Langevin-type equations [27–29], dinuclear system (DNS) model [30–34], etc. Recently, the time-dependent Hartree-Fock (TDHF) method was also applied to investigate the quasifission and fusion-fission dynamics in the reactions of ^{48}Ca+^{239,244}Pu [35]. Modifications of macroscopic models are required for self-consistent and reasonable explanation of fusion dynamics in massive systems. The production cross sections of SHEs $Z = 119$ and 120 were estimated within the multidimensional Langevin-type equations [36] and DNS models [37–42] for different reaction systems. A systematic study on SHN production beyond oganesson ($Z = 118$) is needed to predict the optimal projectile-target combinations and reaction mechanisms.

In this work, stochastic diffusion in the nucleon transfer process is applied to the DNS model via the Monte Carlo procedure. A systematic analysis of the production of new superheavy elements was performed. The remainder of this paper is organized as follows. In Sect. 2 a brief description of the DNS model is presented. A comparison with the available data and predictions of new elements $Z = 119 - 122$ are discussed in Sect. 3. A summary is provided in Sect. 4.

2 Model description

We apply DNS model to the quasi-fission and fusion dynamics, multinucleon transfer reactions, and deep inelastic collisions We assume that the dissipation of the relative motion and rotation of the colliding system into the internal degrees of freedom are at the touching configuration. The DNS system evolves along two main degrees of freedom to form a compound nucleus: the radial motion via the decay of DNS and the nucleon transfer via the mass asymmetry $\eta = (A_1 - A_2)/(A_1 + A_2)$ [43–45]. In accordance with the temporal sequence, the system undergoes capture by overcoming the Coulomb barrier, the competition of quasi-fission and complete fusion by cascade nucleon transfer, and the formation of cold residue nuclide by evaporating γ-rays, neutrons, light charged particles, and binary fission. The production cross section of the superheavy residue is estimated by summing partial waves with angular momentum J at the incident center of mass energy $E_{\mathrm{c.m.}}$ as

$$\sigma_{\mathrm{ER}}(E_{\mathrm{c.m.}}) = \frac{\pi\hbar^2}{2\mu E_{\mathrm{c.m.}}} \sum_{J=0}^{Jmax} (2J+1) T(E_{\mathrm{c.m.}}, J) \times P_{\mathrm{CN}}(E_{\mathrm{c.m.}}, J) W_{\mathrm{sur}}(E_{\mathrm{c.m.}}, J). \quad (1)$$

Here, $T(E_{\mathrm{c.m.}}, J)$ is the penetration probability and is given by a Gaussian-type barrier distribution. The fusion probability P_{CN} is described by the DNS model, considering the competition between the quasi-fission and fission of the heavy fragment. The survival probability W_{sur} was calculated using a statistical approach [46–49].

In the DNS model, the time evolution of the distribution probability $P(Z_1, N_1, E_1, t)$ for fragment 1 with proton number Z_1, neutron number N_1, and excitation energy E_1 are described by the following master equation:

$$\frac{dP(Z_1,N_1,E_1,t)}{dt} = \sum_{Z_1'} W_{Z_1,N_1;Z_1',N_1}(t)[d_{Z_1,N_1}P(Z_1',N_1,E_1',t) - d_{Z_1',N_1}P(Z_1,N_1,E_1,t)] + \sum_{N_1'} W_{Z_1,N_1;Z_1,N_1'}(t) \times [d_{Z_1,N_1}P(Z_1,N_1',E_1',t) - d_{Z_1,N_1'}P(Z_1,N_1,E_1,t)] - [\Lambda^{qf}_{Z_1,N_1,E_1,t}(\Theta) + \Lambda^{fis}_{Z_1,N_1,E_1,t}(\Theta)]P(Z_1,N_1,E_1,t). \quad (2)$$

Here $W_{Z_1,N_1;Z_1',N_1}(W_{Z_1,N_1;Z_1,N_1'})$ is the mean transition probability from the channel(Z_1,N_1,E_1) to (Z_1',N_1,E_1'), [or (Z_1,N_1,E_1) to (Z_1,N_1',E_1')]; d_{Z_1,Z_1} denotes the microscopic dimension corresponding to the macroscopic state (Z_1,N_1,E_1).The sum is taken over all possible proton and neutron numbers that fragment Z_1' and N_1' may take; however, only one nucleon transfer is considered in the model with the relations $Z_1' = Z_1 \pm 1$ and $N_1' = N_1 \pm 1$. The excitation energy E_1 is determined by the dissipation energy from the relative motion and the potential energy surface of the DNS. The quasi-fission rate Λ^{qf} and fission rate Λ^{fis} are given by the one-dimensional Kramers formula [50]. The motion of nucleons in the interacting potential is governed by the single-particle Hamiltonian [32], which is influenced by the local excitation energy of the DNS.

The potential energy surface (PES) of the DNS is given by

$$U(\{\alpha\}) = B(Z_1,N_1) + B(Z_2,N_2) - \left[B(Z,N) + V^{CN}_{rot}(J)\right] + V(\{\alpha\}). \quad (3)$$

The DNS fragments satisfy the relation $Z_1 + Z_2 = Z$ and $N_1 + N_2 = N$, where Z and N are the proton and neutron numbers of the composite system, respectively. The symbol α denotes the quantities of Z_1, N_1, Z_2, N_2, J, R, β_1, β_2, θ_1, θ_2; $B(Z_i,N_i)(i=1,2)$ and $B(Z,N)$ are the negative binding energies of the fragment (Z_i,N_i) and the compound nucleus (Z,N), respectively; V^{CN}_{rot} is the rotational energy of the compound nucleus; β_i represents the quadrupole deformations of the two fragments and is taken as the ground-state values; θ_i denotes the polar angles between the collision orientations and symmetry axes of the deformed nuclei. The collision direction is sampled using the Monte Carlo method with $\theta_i = \frac{\pi}{2}\xi_i$, where ξ_i is a random number. The angles $\theta_i(i=1,2)$ of binary DNS fragments are stochastically sampled; the angles differ in the nucleon transfer process. The interaction potential between fragments (Z_1,N_1) and (Z_2,N_2) includes the nuclear, Coulomb, and centrifugal parts

$$V(\{\alpha\}) = V_N(\{\alpha\}) + \frac{J(J+1)\hbar^2}{2\mu R^2} + V_C(\{\alpha\}), \quad (4)$$

where μ is the reduced mass of the two DNS fragments. The nuclear potential was calculated using the double-folding method based on the Skyrme interaction force without considering the momentum and spin dependence [51]. The Coulomb potential was obtained using Wong's formula [52]. The distance R between the centers of two fragments was chosen as the minimal position of the interaction pocket. The minimal path in the valley of the PES is called the driving potential and is dependent on mass asymmetry. Figure 1 shows the driving potentials for the tip-tip and waist-waist collisions; it also show the average value of random orientations in the reaction of $^{48}Ca + ^{238}U$. The tip-tip orientation indicates that the interaction potential is the minimum when the polar angle θ corresponds to the inner fusion barrier of $B_{fus} = 9.9$ MeV; the waist-waist case is the maximal potential for the DNS fragments with $B_{fus} = 4.8$ MeV. In all orientations, the driving potential exhibits a symmetric structure. The driving potential with random collisions is close to the average values of the tip-tip and waist-waist collisions. The inner fusion barrier is related to the collision orientation; the waist-waist collisions undergo a high barrier to form a compound nucleus. However, the bump structure toward a decrease in mass asymmetry hinders the quasifission process.

In order to form a compound nucleus (CN) overcoming the internal fusion barrier, the DNS must have sufficient local excitation. The formation probability of the compound nucleus at Coulomb barrier B and angular momentum J is given by the summation of the BG point

$$P_{CN}(E_{c.m.},J,B) = \frac{1}{N_t}\sum_{i=1}^{Nt}\sum_{Z_1=1}^{ZB.G.}\sum_{N_1=1}^{NB.G.} \times P(Z_1,N_1,E_1(\theta_1,\theta_2),\tau_{int}(\theta_1,\theta_2)) \times \sin\theta_1 \sin\theta_2. \quad (5)$$

Here, the interaction time $\tau_{int}(E_{c.m.},J,B)$ is obtained using the deflection function method [53]. The excitation energy E_1 of the DNS fragment (Z_1,N_1) is related to the

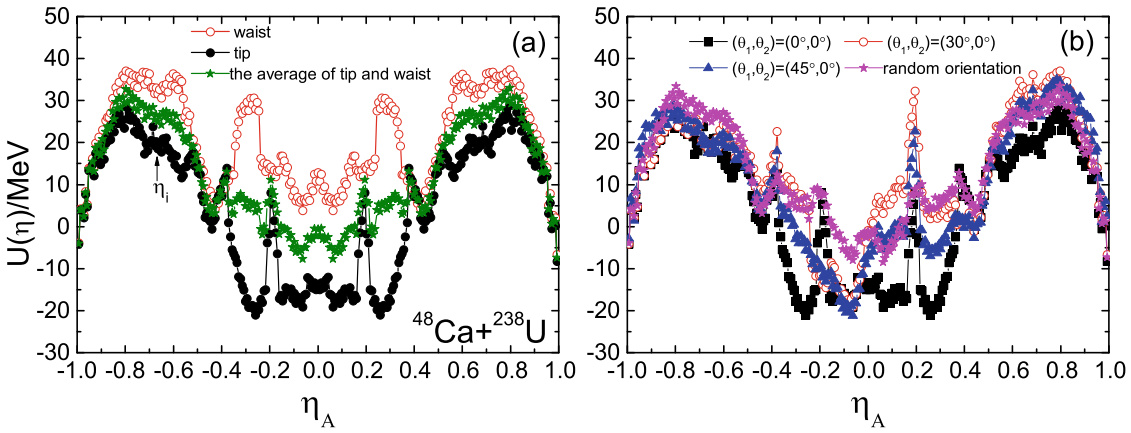

Fig. 1 (Color online) The driving potentials in the reaction of $^{48}Ca+^{238}U$ with the waist-waist, tip-tip, random collisions and fixed angles, respectively

collision orientation θ_1 and θ_2; N_t is the total event for the Monte Carlo integration with $\theta_i = \frac{\pi}{2}\xi$. The fusion probability is calculated using a Gaussian distribution $f(B)$ as

$$P_{\mathrm{CN}}(E_{\mathrm{c.m.}}, J) = \int f(B) P_{\mathrm{CN}}(E_{\mathrm{c.m.}}, J, B)\mathrm{d}B. \tag{6}$$

The collision orientation influences the PES of the DNS because of the different interaction potential with the stochastic angle. Consequently, the formation probability of CN is related to the orientation of the two DNS fragments. Figure 2 shows the dependence of the fusion probability on excitation energy at different orientations in the nucleon transfer process in the reaction of $^{48}Ca+^{238}U$. The fusion probability increases with the excitation energy of the compound nucleus. The waist-waist case leads to a high fusion probability owing to the lower inner fusion barrier and a small peak towards the symmetric diffusion (quasifission path). The statistical error is included for random collisions, in which the fusion probability lies between fixed orientations. Usually, the tip-tip orientation is chosen in the calculation of the fusion probability, which is considered to be a probable nucleon transfer [32].

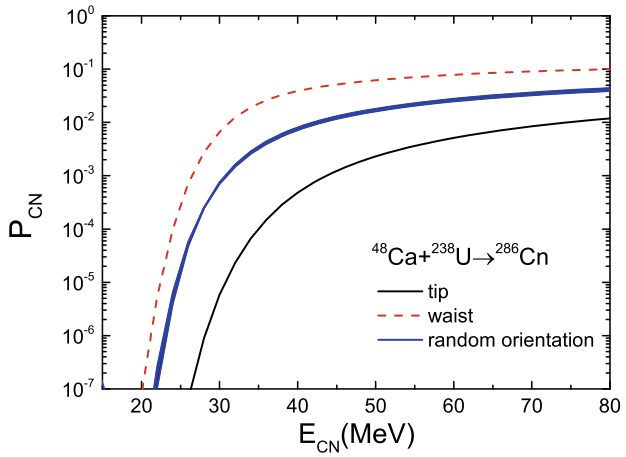

Fig. 2 (Color online) A comparison of the fusion probability a function of excitation energy in the reaction of $^{48}Ca+^{238}U$ at different collision orientations

Once the compound nucleus is formed by cascade nucleon transfer, de-excitation occurs by emitting γ-rays, particles (n, p, d, α, etc.), and binary fission. The survival probability of heavy nuclei after evaporating particles is crucial for assessing cross sections, which is usually calculated using a statistical process. The probability in the channel for evaporating the x-th neutron, y-th proton, and zth-α is expressed as [46]

$$W_{\mathrm{sur}}(E^*_{\mathrm{CN}}, x, y, z, J) = P(E^*_{\mathrm{CN}}, x, y, z, J) \times \prod_{i=1}^{x} \frac{\Gamma_{\mathrm{n}}(E^*_i, J)}{\Gamma_{\mathrm{tot}}(E^*_i, J)} \prod_{j=1}^{y} \frac{\Gamma_{\mathrm{p}}(E^*_j, J)}{\Gamma_{\mathrm{tot}}(E^*_j, J)} \prod_{k=1}^{z} \frac{\Gamma_{\alpha}(E^*_k, J)}{\Gamma_{\mathrm{tot}}(E^*_k, J)}. \tag{7}$$

Here, E^*_{CN}, J, and Γ_{tot} are the excitation energy, spin of the compound nucleus, and sum of partial widths of particle evaporation, respectively. The excitation energy E^*_s before evaporating the sth particles is given by:

$$E^*_{s+1} = E^*_s - B^{\mathrm{n}}_i - B^{\mathrm{p}}_j - B^{\alpha}_k - 2T_s, \tag{8}$$

with the initial value $E^*_1 = E^*_{\mathrm{CN}}$ and $s = i + j + k$. The nuclear temperature T_i is given by $E^*_i = aT_i^2 - T_i$, where a is the level density parameter. The widths of the neutron evaporation and fission are calculated using the Weisskopf evaporation theory. The fission barrier is evaluated from the macroscopic liquid drop model and shell correction energy and is given as

$$B_{\mathrm{f}}(E^*, J) = B^{\mathrm{LD}}_{\mathrm{f}} + E_{\mathrm{shell}} \exp(-E^*/E_{\mathrm{D}}), \tag{9}$$

where the macroscopic part B_f^{LD} is calculated using the liquid drop model. The microcosmic shell correction energy is calculated using the Strutinsky method obtained from Ref. [54]. The damping energy E_D is associated with the level density and mass number of the compound nucleus; the shell correction and excitation energy dependence are considered in the calculation [46].

3 Results and discussion

The production rate of SHNs in massive fusion reactions is significantly low owing to the fusion hindrance in heavy systems, which enables the quasifission process in binary collisions. The evaporation residue (ER) excitation functions in different channels favor experimental measurements with optimal projectile-target combinations and suitable beam energies. The reaction dynamics in the competition of quasifission and fusion-fission reactions, level density, separation energy of evaporated particles, and fission barrier of the compound nucleus influence the ER cross sections. Figure 3 shows the ER excitation functions in the reaction of ^{48}Ca+^{238}U; the results are compared with the data from Dubna [55]. The ER cross sections for producing SHN significantly depend on the orientations of both DNS fragments in the nucleon transfer process. The tip-tip collisions have lower cross sections that the waist-waist orientations and approximately lead to a two-order reduction because of the higher inner fusion barrier for merging the compound nucleus. The cross sections with the stochastic selection of the collision angle of two DNS fragments lie between the tip-tip and waist-waist orientation. The results with tip-tip collisions are consistent with the available data; this results were chosen in the calculation. The formation probabilities of compound nuclei in the fusion reactions are mainly determined by the inner fusion barrier and quasifission barrier (the height of the potential pocket), which correspond to 9.9 MeV (4.8 MeV) and 2.43 MeV (2.41 MeV) in the tip-tip (waist-waist) collisions. The lower inner fusion barrier and higher quasifission barrier are favorable for compound nucleus formation. The maximal yield of SHN ^{283}Cn with 3 pb is positioned in the 3n channel via tip-tip collisions at an excitation energy of 35 MeV. The SHN was still far from the neutron shell closure ($N = 184$). A new reaction mechanism is expected to create a neutron-rich SHN. Pure neutron channels are the dominant decay modes for surviving SHN. The cross sections with mixed channels of protons and α were reduced by two orders of magnitude with the 3 particle channels, for example, p2n and α2n. The charged particle channels and isospin diffusion are important for producing proton-rich actinide nuclides close to the drip line in the fusion-evaporation reactions and multinucleon transfer dynamics [56, 57].

Superheavy elements from Fl ($Z = 114$) to Og ($Z = 118$) were successfully synthesized with ^{48} Ca-induced reactions on actinide targets. This manifests a strong shell effect in the production and decay chains. Figure 4 shows the ER excitation functions for producing superheavy elements 114-118 with ^{244}Pu, ^{248}Cm, ^{249}Bk, and ^{249}Cf as the targets. Different evaporation channels are

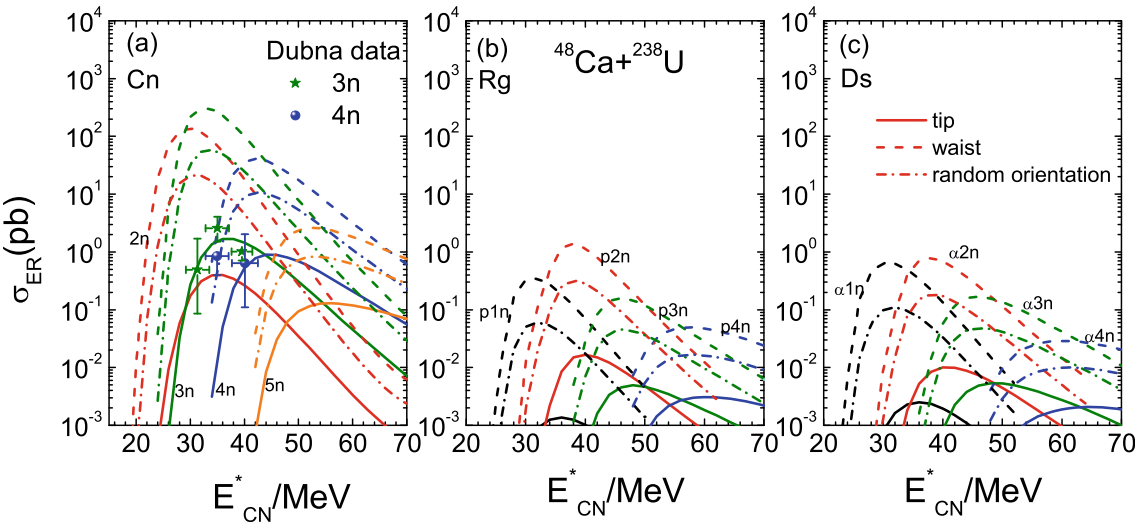

Fig. 3 (Color online) Calculated ER cross sections with different channels of (2-5)n, 1p(2-4)n and 1α(1-3)n and compared with the experimental data in the reaction of ^{48}Ca+^{238}U [55]

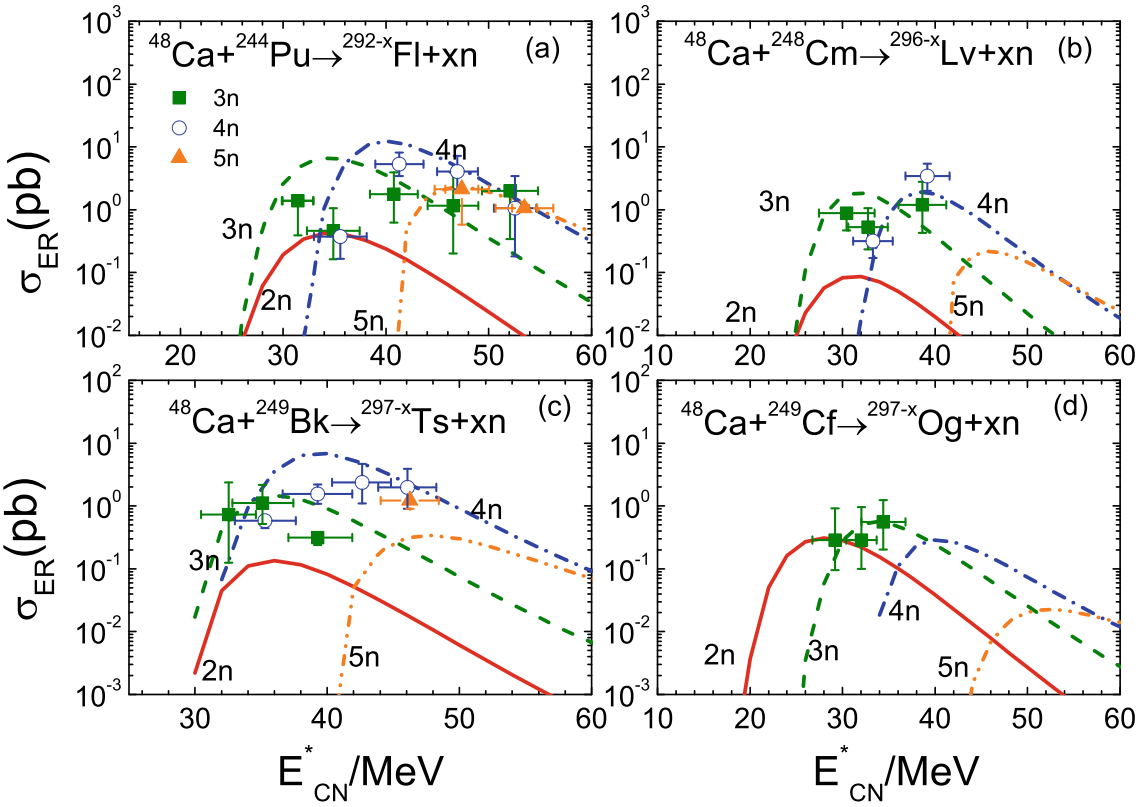

Fig. 4 (Color online) ER excitation functions with pure neutron channels and compared with the experimental data in the reactions of ^{48}Ca+^{244}Pu, ^{248}Cm, ^{249}Bk, ^{249}Cf [55, 58]

distinguished by colored lines and compared with experimental data [55, 58]. The 3n and 4n channels are the dominant decay modes for SHN production. The 2n channel is pronounced with an increase in the charge number of the SHN. However, the cross sections in the 4n and 5n channels decrease with increasing SHN. Unlike the cold fusion reactions, the maximal cross section in the ^{48}Ca induced reactions weakly depends on the mass of ER nucleus, e.g., the value of 8 pb for ^{288}Fl and 0.6 pb for ^{294}Og. The construction of the target material for the synthesis of new SHNs is a challenge. The hot fusion reactions also provide a possible way to create new elements in the eighth period with projectiles ^{45}Sc, ^{50}Ti, ^{54}Cr, ^{58}Fe, ^{64}Ni, etc. In addition to the reaction dynamics in the formation of SHN in hot fusion reactions, nuclear structure effects, such as shell effect, neutron separation energy, odd-even effect, microscopic state of compound nucleus (isomeric state), etc., are important in the evaluation of the production cross section.

Attempts to synthesize superheavy elements 119 and 120 were made at different laboratories worldwide, for

Table 1 Optimal evaporation residual cross sections via different reactions leading to the formation of SHE $Z = 119$

Reaction systems	σ_{ER} (pb)	E^*_{CN} (MeV)	References
^{249}Bk(^{50}Ti,3n)^{296}119	0.04	41	[59]
^{249}Bk(^{50}Ti,4n)^{295}119	0.06	44	[59]
^{254}Es(^{48}Ca,3n)^{299}119	0.3	35	[60]
^{252}Es(^{48}Ca,4n)^{296}119	0.2	43	[61]
^{254}Es(^{48}Ca,4n)^{298}119	0.015	41	[61]
^{249}Bk(^{50}Ti,4n)^{295}119	0.03	36	[61]
^{249}Bk(^{50}Ti,3n)^{296}119	0.035	27	[40]
^{249}Bk(^{50}Ti,4n)^{295}119	0.11	39	[40]
^{249}Bk(^{50}Ti,4n)^{295}119	0.57	41	[62]
^{252}Es(^{44}Ca,3n)^{293}119	4.32	35	[41]
^{251}Cf(^{45}Sc,3n) ^{293}119	0.38	37	This work
^{249}Cf(^{45}Sc,3n)^{291}119	0.99	37	
^{247}Bk(^{50}Ti,4n)^{293}119	0.024	45	
^{249}Bk(^{50}Ti,4n)^{295}119	0.013	45	

example, FLNR, GSI, GANIL, etc. However, no decay chains were observed in these experiments. Theoretical predictions with various models were also made to produce the element 119 with a number of systems, for example, ^{249}Cf (^{45}Sc,xn) $^{294-x}$119, ^{251}Cf (^{45}Sc,xn) $^{296-x}$119, ^{247}Bk (^{50}Ti,xn) $^{297-x}$119, ^{249}Bk (^{50}Ti,xn) $^{299-x}$119, ^{254}Es(^{48}Ca,xn)$^{302-x}$119. Some results for the optimal ER cross sections in different reactions leading to the formation of $Z = 119$ are listed in Table 1. The optimal system of ^{252}Es (^{44}Ca,3n) ^{293}119 is possible with a larger cross section of 4 bps by the DNS model [41]. Further confirmation of the reliability of the calculation through different models is required. However, constructing the target material ^{252}Es in experiments is significantly difficult. The reaction of ^{45}Sc+^{249,251}Cf is also feasible for synthesizing a new element with a cross section above 0.1 pb. Difference of one order magnitude for producing the element 119 in the reaction ^{50}Ti+^{249}Bk exists in the model predictions, for example, 0.03 pb in the 4n channel at the excitation energy of 36 MeV by the FBD model [61], 0.57 pb at 41 MeV by the diffusion model with Langevin-type equations [62], 0.11 pb in Ref. [40], and 0.013 pb in our calculation by the DNS model. The 3n and 4n channels are optimal ways to create the new element, as shown in Fig. 5. The isotopic dependence of the ER cross sections is weak. A larger mass asymmetry in the bombarding system was favorable for producing SHN. The synthesis of element 119 in laboratories is possible in future experiments with high-intensity accelerators worldwide. Reliable predictions in theories are helpful for experimental management.

The synthesis of superheavy element 120 is particularly important for understanding the shell structure in the domain of SHNs. The strong shell effect enhances the fission barrier and α decay half-life, which is favorable for producing and surviving SHN. A possible experiment is planned at HIAF with high-intensity beams. Figure 6 shows a systematic comparison for producing SHN of $Z = 120$ with actinide nuclide-based reactions; different panels represent different reaction systems to create the superheavy element 120 with different neutron richness. The compound nuclei formed by different combinations were close to the neutron shell closure ($N = 184$). Channels 2, 3, and 4n were available for SHN production with excitation energies of approximately 25, 30, and 40 MeV, respectively. The maximal ER cross section depends on the isotopic projectiles. The 3n channel of the ^{44,45}Sc + ^{252}Es reaction is favorable for synthesizing the new SHN owing to the large mass asymmetry in the entrance system. A

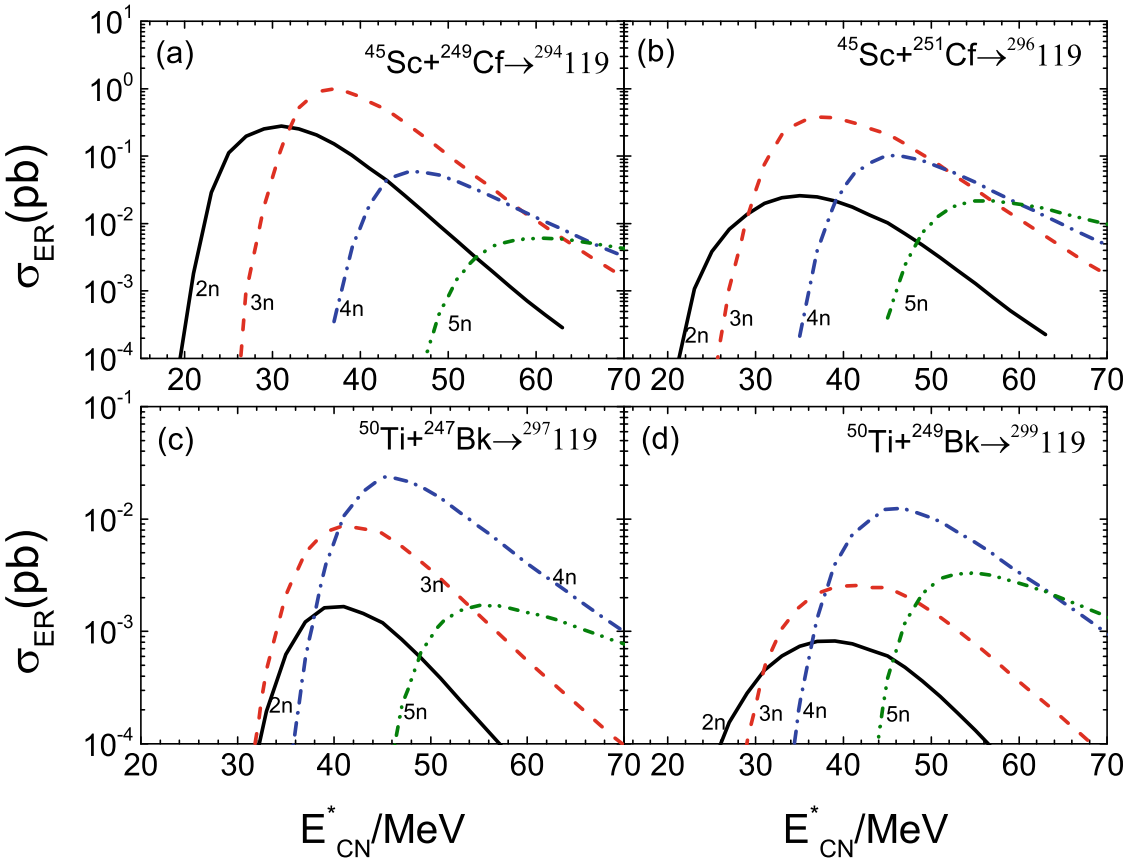

Fig. 5 The evaporation residue cross sections with channels of (2-5)n of element $Z = 119$ in collisions by different reactions

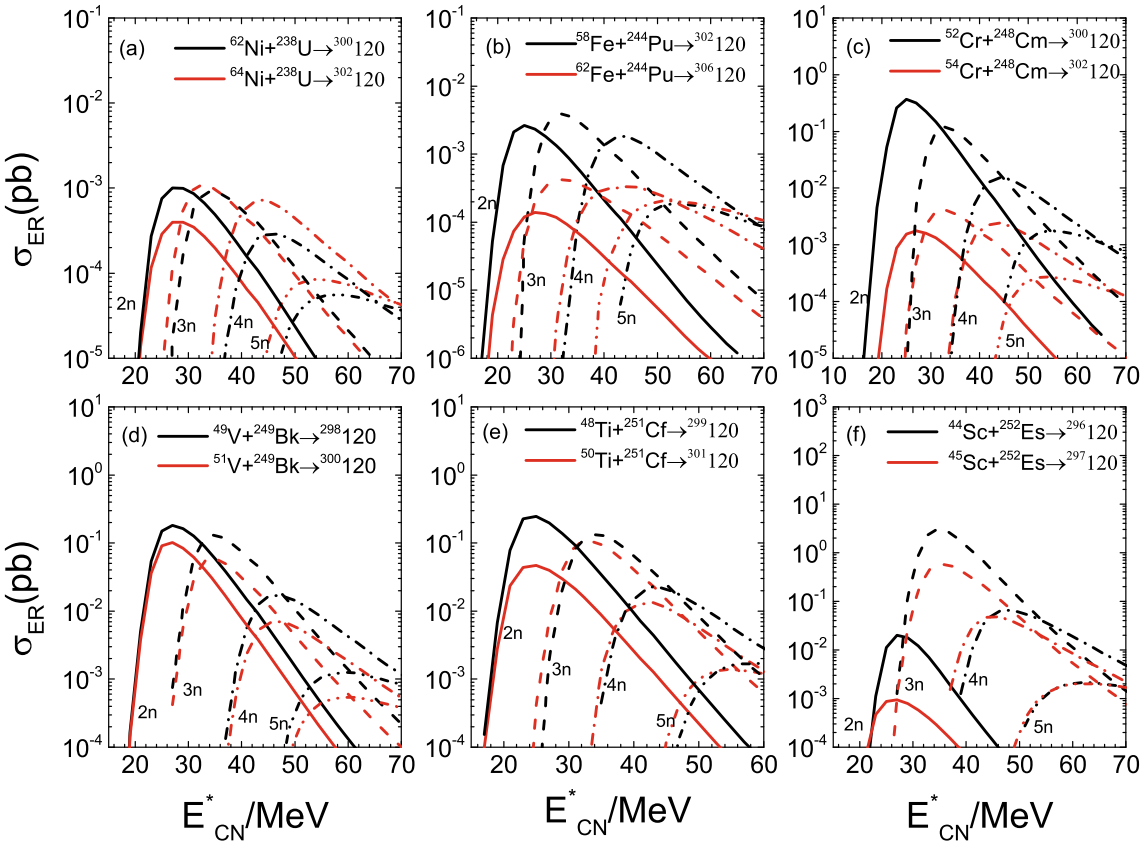

Fig. 6 (Color online) The same as in Fig. 5; for the production of element $Z = 120$

smaller neutron separation energy is available for cooling the compound nuclei formed during the fusion reactions. In Table 2, the production cross sections of $Z = 120$ with the optimal channels and possible combinations are compared. Differences in model predictions exist in the calculations, for example, the production of ^{295}120 in collisions of ^{50}Ti on ^{249}Cf of 0.006 pb and 0.046 pb by the FBD model [61] and multidimensional Langevin-type equations [59], respectively. Calculations support the 3n channel in collisions of ^{50}Ti on californium isotopes is available for synthesizing the element 120 with the cross section above 0.1 pb at the excitation energy of approximately 35 MeV. The 2n channel in the reactions of ^{49,51}V+^{249}Bk can also create a new element. The position of the maximal cross section is mainly determined by the odd-even effect of neutron evaporation and the energy dependence of the fusion probability. Note that the proton shell closure $Z = 120$ was predicted with the relativistic mean-field model by including the isospin dependence of the spin-orbit interaction and the effective mass [65]. The shell correction energy calculated by the macroscopic-microscopic model is used in the calculation, and the $Z = 114$ proton shell closure is given by the approach [54]. The production cross section of element 120 is enhanced with shell correction by the relativistic mean-field model.

As an extension of the model prediction, we analyzed the formation of superheavy elements 121 and 122 in massive fusion reactions. Figure 7 shows the ER excitation functions in the reactions of ^{54}Cr+^{247,249}Bk and ^{58,64}Fe+^{243}Am; in panels (a) and (b), the stable nuclide ^{54}Cr and isotopic target nuclei are selected. The (2–4)n channels in the ^{54}Cr+^{249}Bk reaction are favorable with significantly low cross sections at the level of 1 fb; The influence of stable and radioactive nuclides on SHN production is compared in panels (c) and (d). The different structure of (2–5)n channels is caused by the neutron separation energy in the cascade evaporation, that is, the smaller separation energy for the compound nucleus

Table 2 The same as in Table 1; for the production of SHE $Z = 120$

Reaction systems	σ_{ER} (pb)	E^*_{CN} (MeV)	References
^{249}Cf(^{50}Ti,4n)^{295}120	0.006	43	[61]
^{251}Cf(^{50}Ti,4n)^{297}120	0.003	42	
^{248}Cm(^{54}Cr,4n)^{298}120	0.001	35	
^{244}Pu(^{58}Fe,3n)^{299}120	0.01	36	[63]
^{238}U(^{64}Ni,3n)^{299}120	0.007	36	
^{248}Cm(^{54}Cr,3n)^{299}120	0.076	36	
^{249}Cf(^{50}Ti,3n)^{296}120	0.76	33	
^{249}Cf(^{50}Ti,3n)^{296}120	0.1	29	[64]
^{248}Cm(^{54}Cr,3n)^{299}120	0.055	30	
^{249}Cf(^{50}Ti,4n)^{295}120	0.046	43	[59]
^{248}Cm(^{54}Cr,4n)^{298}120	0.028	43	
^{249}Cf(^{50}Ti,3n)^{296}120	0.06	36	[29]
^{250}Cf(^{50}Ti,3n)^{297}120	0.12	37	
^{251}Cf(^{50}Ti,4n)^{297}120	0.11	38	
^{252}Cf(^{50}Ti,4n)^{298}120	0.25	38	
^{251}Cf(^{50}Ti,3n)^{298}120	0.25	36	[40]
^{249}Cf(^{50}Ti,3n)^{296}120	0.05	33	
^{248}Cm(^{54}Cr,4n)^{298}120	0.005	42	
^{244}Pu(^{58}Fe,4n)^{298}120	0.003	43	
^{249}Cf(^{50}Ti,3n)^{296}120	0.02	31	
^{257}Fm(^{40}Ca,3n)^{294}120	1.24	48	[41]
^{248}Cf(^{46}Ti,2n)^{292}120	0.17	34	
^{249}Cf(^{46}Ti,3n)^{292}120	0.24	39	
^{250}Cf(^{46}Ti,2n)^{294}120	0.13	36	
^{251}Cf(^{46}Ti,3n)^{294}120	0.37	39	
^{251}Cf(^{50}Ti,3n)^{298}120	0.11	33	This work
^{251}Cf(^{48}Ti,2n)^{297}120	0.25	25	
^{244}Pu(^{58}Fe,3n)^{299}120	0.004	33	
^{244}Pu(^{62}Fe,3n)^{303}120	0.0004	31	
^{248}Cm(^{54}Cr,3n)^{299}120	0.004	33	
^{248}Cm(^{52}Cr,2n)^{300}120	0.37	25	
^{238}U(^{64}Ni,3n)^{299}120	0.001	31	
^{238}U(^{62}Ni,2n)^{300}120	0.001	27	
^{252}Es(^{44}Sc,3n)^{293}120	3.18	35	
^{252}Es(^{45}Sc,3n)^{293}120	0.59	35	
^{249}Bk(^{49}V,2n)^{296}120	0.18	27	
^{249}Bk(^{51}V,2n)^{298}120	0.1	27	

^{301}121, resulting in a larger 2n channel probability. The production cross section of element 122 is significantly low in the fusion reactions, as shown in Fig. 8. The neutron separation energy and fission barrier are sensitive to the survival of the SHN. The polar angle distribution, mass, total kinetic energy spectra, and excitation energy dependence of fission fragments from the SHNs are useful for extracting the fission barrier and shell evolution. Further experiments are required in the future. The systems of ^{54}Cr+ ^{249,251}Cf and ^{58,64}Fe+^{248}Cm were chosen to synthesize element 122, as shown in Fig. 8. The cross section below 0.1 fb is out of the limit of the experimental measurement. The new reaction mechanism is expected for creating the neutron-rich SHN and new element, i.e., the

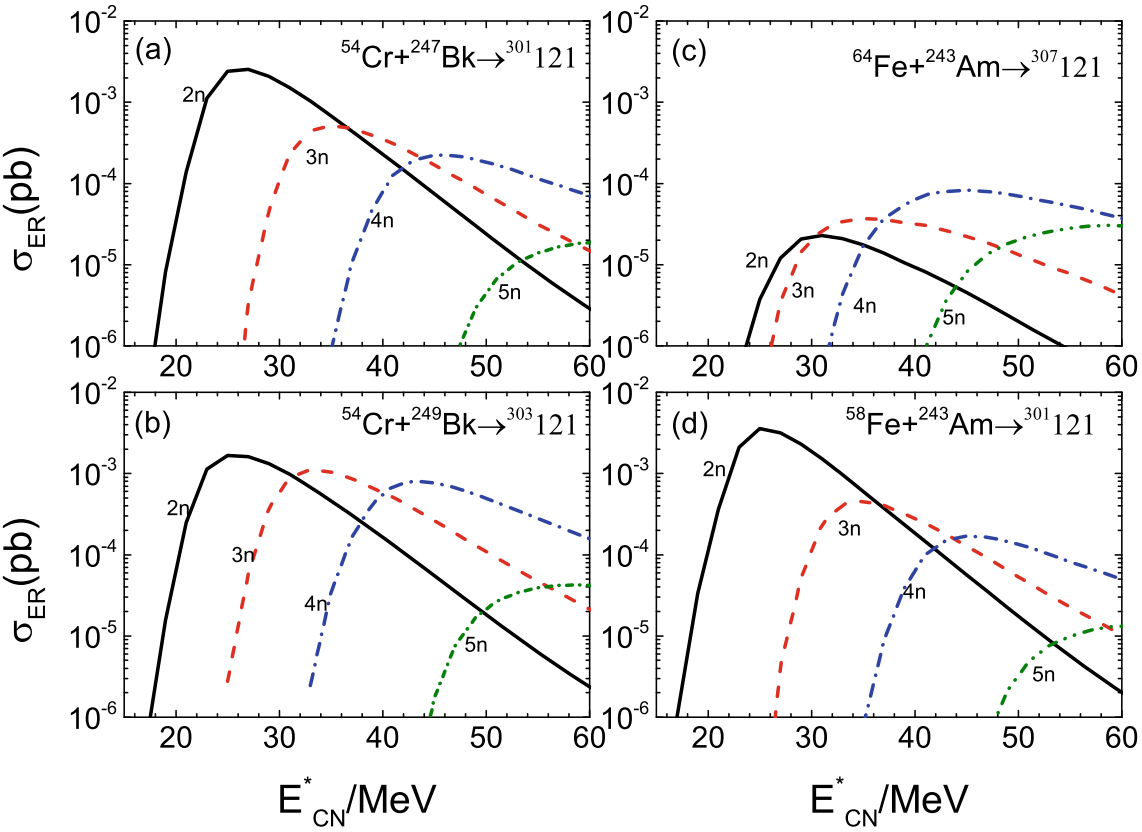

Fig. 7 (Color online) The evaporation residue cross sections with channels of (2-5)n of element $Z = 121$ in collisions by different combinations

multinucleon transfer reaction, incomplete fusion with radioactive nuclide, etc.

4 Conclusion

Within the framework of the DNS model, SHN formation in the fusion-evaporation reactions was thoroughly investigated. Stochastic collision orientations in the nucleon transfer process were implemented into the model via the Monte Carlo approach. The calculated results are consistent with the experimental data from Dubna. The maximal cross sections of the evaporation residues appear in the (2-5)n evaporation channels. The yields in the 1pxn, 1αxn, and 1p1αxn evaporation channels are significantly lower than those of pure neutron evaporation. The reactions of ^{249}Cf $(^{45}$Sc,xn$)^{294-x}$119, ^{251}Cf$(^{45}$Sc,xn$)^{296-x}$119, ^{247}Bk$(^{50}$Ti,xn$)$ $^{297-x}$119, and ^{249}Bk$(^{50}$Ti,xn$)^{299-x}$119 were investigated to synthesize the new element 119. We conclude that the maximum cross sections are close to 1 pb in the 3n evaporation channel for the systems and weakly depend on the isotopic target nucleus. The synthesis of the element $Z = 120$ was investigated using a series of isotopic projectile nuclei bombarding actinide targets. The optimal combination is the reaction of ^{44}Sc+^{252}Es in the 3n channel with a cross section of 3 pb. The production of superheavy elements 121 and 122 was obtained at a level below 1 fb in the massive fusion reactions. A new reaction mechanism

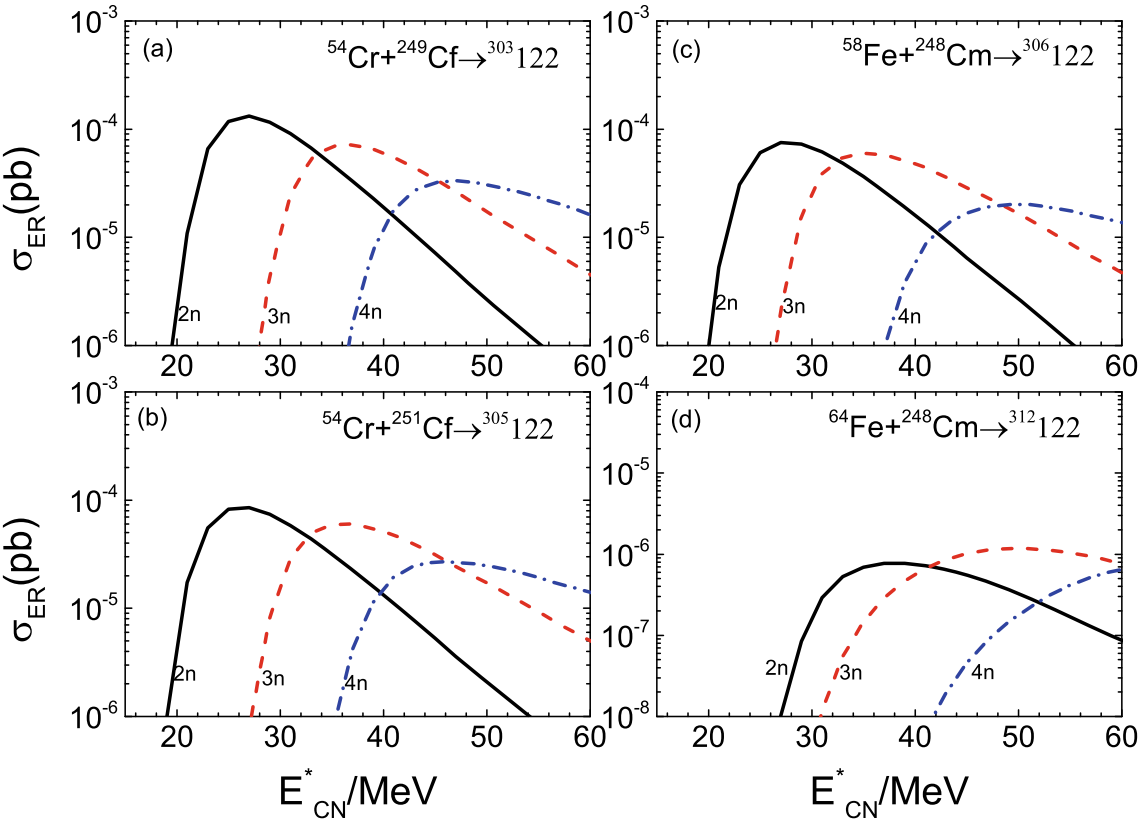

Fig. 8 (Color online) The same as in Fig. 5; for the production of element $Z = 122$

still needs to be explored for the production of new elements. Therefore, the synthesis of new SHNs in experiments provides a good theoretical basis for selecting collision combinations.

Author Contributions All authors contributed to the study conception and design. Material preparation, data collection and analysis were performed by Fei Niu, Peng-Hui Chen and Zhao-Qing Feng. The first draft of the manuscript was written by Fei Niu, Peng-Hui Chen and Zhao-Qing Feng and all authors commented on previous versions of the manuscript. All authors read and approved the final manuscript.

References

1. Y. T. Oganessian, F.S. Abdullin, P.D. Bailey et al., Synthesis of a new element with atomic number Z=117. Phys. Rev. Lett. **104**, 142502 (2010). 10.1103/PhysRevLett.104.142502
2. A. Sobiczewski, F.A. Gareev, B.N. Kalinkin, Closed shells for Z> 82 and N > 126 in a diffuse potential well. Phys. Lett. **22**, 500 (1966). https://doi.org/10.1016/0031-9163(66)91243-1
3. Z.Q. Feng, Nuclear dynamics and particle production near threshold energies in heavy-ion collisions. Nucl. Sci. Tech. **29**, 40 (2018). https://doi.org/10.1007/s41365-018-0379-z
4. A. Sobiczewski, K. Pomorski, Description of structure and properties of superheavy nuclei. Prog. Part. Nucl. Phys. **58**, 292 (2007). https://doi.org/10.1016/j.ppnp.2006.05.001
5. S. Ćwiok, P.-H. Heenen, W. Nazarewicz, Shape coexistence and triaxiality in the superheavy nuclei. Nature (London) **433**, 705 (2005). https://doi.org/10.1038/nature03336
6. S. Hofmann, D. Ackermann, S. Antalic et al., Probing shell effects at Z= 120 and N= 184. GSI Scientific Report-2007, 131 (2008)
7. Y. T. Oganessian, V.K. Utyonkov, Yu.V. Lobanov et al., Attempt to produce element 120 in the $^{244}Pu+^{58}Fe$ reaction. Phys. Rev. C **79**, 024603 (2009). https://doi.org/10.1103/PhysRevC.79.024603
8. S. Hofmann et al., Physics experiments on superheavy elements at the GSI SHIP. GSI Scientific Report-2011, 205 (2012)
9. S. Hofmann, S. Heinz, R. Mann et al., Review of even element super-heavy nuclei and search for element 120. Eur. Phys. J. A **52**, 180 (2016). https://doi.org/10.1140/epja/i2016-16180-4
10. J. Khuyagbaatar, A. Yakushev, E. Ch, *Dullmann et al., The Superheavy Element Search Campaigns at TASCA* (GSI Scientific Report-2012, 2013), p. 131
11. H.M. Albers, J. Khuyagbaatar, D.J. Hinde et al., Zeptosecond contact times for element $Z = 120$ synthesis. Phys. Lett. B **808**, 135626 (2020). https://doi.org/10.1016/j.physletb.2020.135626
12. E.K. Hulet, R.W. Lougheed, J.F. Wild et al., Search for superheavy elements in the bombardment of ^{248}Cm with ^{48}Ca. Phys. Rev. Lett. **39**, 385 (1977). https://doi.org/10.1103/PhysRevLett.39.385
13. M. Schädel, J.V. Kratz, H. Ahrens et al., Isotope distributions in the reaction of ^{238}U with ^{238}U. Phys. Rev. Lett. **41**, 469 (1978). https://doi.org/10.1103/PhysRevLett.41.469
14. Y. T. Oganessian, A.S. Iljnov, A.G. Demin et al., Experiments on the production of fermium neutron-deficient isotopes and new possibilities of synthesizing elements with Z > 100. Nucl. Phys.

A **239**, 353 (1975). https://doi.org/10.1016/0375-9474(75)90456-X
15. Y. T. Oganessian, A.S. Iljnov, A.G. Demin et al., Experiments on the synthesis of neutron-deficient kurchatovium isotopes in reactions induced by ^{50}Ti Ions. Nucl. Phys. A **239**, 157 (1975). https://doi.org/10.1016/0375-9474(75)91140-9
16. S. Hofmann, G. Münzenberg, Discovery of the heaviest elements. Rev. Mod. Phys. **72**, 733 (2000). https://doi.org/10.1103/RevModPhys.72.733
17. G. Münzenberg, From bohrium to copernicium and beyond SHE research at SHIP. Nucl. Phys. A **944**, 5 (2015). https://doi.org/10.1016/j.nuclphysa.2015.06.008
18. K. Morita, K. Morimoto, D. Kaji et al., Production and decay properties of ^{272}111 and its daughter nuclei. J. Phys. Soc. Jpn. **73**, 2593 (2004). https://doi.org/10.1143/JPSJ.73.1738
19. Y. T. Oganessian, A.V. Yeremin, A.G. Popeko et al., Synthesis of nuclei of the superheavy element 114 in reactions induced by ^{48}Ca. Nature (London) **400**, 242 (1999). https://doi.org/10.1038/22281
20. Y. T. Oganessian, V.K. Utyonkov, Yu.V. Lobanov et al., Synthesis of superheavy nuclei in the ^{48}Ca+^{244}Pu reaction: ^{288}114. Phys. Rev. C **62**, 041604(R) (2000). https://doi.org/10.1103/PhysRevC.62.041604
21. Y. T. Oganessian, V.K. Utyonkov, Yu.V. Lobanov et al., Synthesis of the isotopes of elements 118 and 116 in the ^{249}Cf and ^{245}Cm+^{48}Ca fusion reactions. Phys. Rev. C **74**, 044602 (2006). https://doi.org/10.1103/PhysRevC.74.044602
22. Y. T. Oganessian, V.K. Utyonkov, Superheavy nuclei from ^{48}Ca-induced reactions. Nucl. Phys. A **944**, 62 (2015). https://doi.org/10.1016/j.nuclphysa.2015.07.003
23. Z.Y. Zhang, Z.G. Gan, L. Ma et al., Observation of the Superheavy Nuclide ^{271}Ds. Chin. Phys. Lett. **29**, 012502 (2012). https://doi.org/10.1088/0256-307X/29/1/012502
24. S. Bjornholm, W.J. Swiatecki, Dynamical aspects of nucleus-nucleus collisions. Nucl. Phys. A **391**, 471 (1982). https://doi.org/10.1016/0375-9474(82)90621-2
25. W.J. Swiatecki, K. Siwek-Wilczynska, J. Wilczynski, Fusion by diffusion II. Synthesis of transfermium elements in cold fusion reactions. Phys. Rev. C **71**(2005). https://doi.org/10.1103/PhysRevC.71.014602
26. T. Cap, K. Siwek-Wilczynska, J. Wilczynski, Nucleus-nucleus cold fusion reactions analyzed with the l-dependent fusion by diffusion model. Phys. Rev. C **83**, 054602 (2011). https://doi.org/10.1103/PhysRevC.83.054602
27. V. Zagrebaev, W. Greiner, Low-energy collisions of heavy nuclei: dynamics of sticking, mass transfer and fusion. J. Phys. G **34**(1), 1 (2007). https://doi.org/10.1088/0954-3899/34/1/001
28. V. Zagrebaev, W. Greiner, New way for the production of heavy neutron-rich nuclei. J. Phys. G **35**, 125103 (2008). https://doi.org/10.1088/0954-3899/35/12/125103
29. Z.H. Liu, J.D. Bao, Role of the coupling between neck and radial degrees of freedom in evolution from dinucleus to mononucleus. Phys. Rev. C **83**, 044613 (2011). https://doi.org/10.1103/PhysRevC.83.044613
30. G.G. Adamian, N.V. Antonenko, W. Scheid et al., Treatment of competition between complete fusion and quasifission in collisions of heavy nuclei. Nucl. Phys. A **627**, 361 (1997). https://doi.org/10.1063/1.55172
31. G.G. Adamian, N.V. Antonenko, W. Scheid et al., Fusion cross sections for superheavy nuclei in the dinuclear system concept. Nucl. Phys. A **633**, 409 (1998). https://doi.org/10.1016/S0375-9474(98)00124-9
32. Z.Q. Feng, G.M. Jin, F. Fu et al., Production cross sections of superheavy nuclei based on dinuclear system model. Nucl. Phys. A **771**, 50 (2006). https://doi.org/10.1016/j.nuclphysa.2006.03.002
33. Z.Q. Feng, G.M. Jin, J.Q. Li et al., Formation of superheavy nuclei in cold fusion reactions. Phys. Rev. C **76**, 044606 (2007). https://doi.org/10.1103/PhysRevC.76.044606
34. Z.Q. Feng, G.M. Jin, J.Q. Li, Dynamics in production of superheavy nuclei in low-energy heavy-ion collisions. Nucl. Phys. Rev. **28**, 1 (2011) https://doi.org/10.11804/NuclPhysRev.28.01.001
35. L. Guo, C. Shen, C. Yu et al., Isotopic trends of quasifission and fusion-fission in the reactions ^{48}Ca+^{239,244}Pu. Phys. Rev. C **98**, 064609 (2018). https://doi.org/10.1103/PhysRevC.98.064609
36. V.I. Zagrebaev, W. Greiner, Cross sections for the production of superheavy nuclei. Nucl. Phys. A **944**, 257 (2015). https://doi.org/10.1016/j.nuclphysa.2015.02.010
37. A.K. Nasirov, G. Giardina, G. Mandaglio et al., Quasifission and fusion-fission in reactions with massive nuclei: Comparison of reactions leading to the Z=120 element. Phys. Rev. C **79**, 024606 (2009). https://doi.org/10.1103/PhysRevC.79.024606
38. Z.Q. Feng, G.M. Jin, J.Q. Li et al., Production of heavy and superheavy nuclei in massive fusion reactions. Nucl. Phys. A **816**, 33 (2009). https://doi.org/10.1016/j.nuclphysa.2008.11.003
39. Z.G. Gan, X.H. Zhou, M.H. Huang et al., Predictions of synthesizing element 119 and 120. Sci. China Phys. Mech. Astron. **54**, s61 (2011). https://doi.org/10.1007/s11433-011-4436-4
40. N. Wang, E.G. Zhao, W. Scheid, Theoretical study of the synthesis of superheavy nuclei with Z=119 and 120 in heavy-ion reactions with transuranium targets. Phys. Rev. C **85**, 041601(R) (2012). https://doi.org/10.1103/PhysRevC.85.041601
41. F. Li, L. Zhu, Z.H. Wu et al., Predictions for the synthesis of superheavy elements Z=119 and 120. Phys. Rev. C **98**, 014618 (2018). https://doi.org/10.1103/PhysRevC.98.014618
42. G.G. Adamian, N.V. Antonenko, H. Lenske et al., Predictions of identification and production of new superheavy nuclei with Z=119 and 120. Phys. Rev. C **101**, 034301 (2020). https://doi.org/10.1103/PhysRevC.101.034301
43. G.G. Adamian, N.V. Antonenko, A. Diaz-Torres, S. Heinz, How to extend the chart of nuclides? Eur. Phys. J. A **56**, 47 (2020). https://doi.org/10.1140/epja/s10050-020-00046-7
44. Z.Q. Feng, G.M. Jin, J.Q. Li, Production of new superheavy Z=108-114 nuclei with ^{238}U, ^{244}Pu and ^{248,250}Cm targets. Phys. Rev. C **80**, 057601 (2009). https://doi.org/10.1103/PhysRevC.80.057601
45. Z.Q. Feng, Production of neutron-rich isotopes around N=126 in multinucleon transfer reactions. Phys. Rev. C **95**, 024615 (2017). https://doi.org/10.1103/PhysRevC.95.024615
46. P.H. Chen, Z.Q. Feng, F. Niu et al., Production of proton-rich nuclei around Z = 84–90 in fusion-evaporation reactions. Eur. Phys. J. A **53**, 9 (2017). https://doi.org/10.1140/epja/i2017-12281-x
47. P.H. Chen, Z.Q. Feng, J.Q. Li et al., A statistical approach to describe highly excited heavy and superheavy nuclei. Chin. Phys. C **40**, 091002 (2016). https://doi.org/10.1088/1674-1137/40/9/091002
48. P.H. Chen, F. Niu, Y.F. Guo et al., Nuclear dynamics in multinucleon transfer reactions near Coulomb barrier energies. Nucl. Sci. Tech. **29**, 185 (2018). https://doi.org/10.1007/s41365-018-0521-y
49. F. Niu, P.H. Chen, H.G. Cheng et al., Multinucleon transfer dynamics in nearly symmetric nuclear reactions. Nucl. Sci. Tech. **31**, 59 (2020). https://doi.org/10.1007/s41365-020-00770-1
50. G.G. Adamian, N. Antonenko, W. Scheid, Characteristics of quasifission products within the dinuclear system model. Phys. Rev. C **68**, 034601 (2003). https://doi.org/10.1103/PhysRevC.68.034601

51. G.G. Adamian, N.V. Antonenko, R.V. Jolos et al., Effective nucleus-nucleus for calculation of potential energy of a dinuclear system. Int. J. Mod. Phys. E **5**, 191 (1996). https://doi.org/10.1142/S0218301396000098
52. C.Y. Wong, Interaction barrier in charged-particle nuclear reactions. Phys. Rev. Lett. **31**, 766 (1973). https://doi.org/10.1103/PhysRevLett.31.766
53. J.Q. Li, G..W. olschin, Distribution of the dissipated angular momentum in heavy-ion collisions. Phys. Rev. C **27**, 590 (1983). https://doi.org/10.1103/PhysRevC.27.590
54. P. Möller et al., Nuclear ground-state masses and deformations. At. Data Nucl. Data Tables **59**, 185 (1995). https://doi.org/10.1006/adnd.1995.1002
55. Y.T. Oganessian, V.K. Utyonkov, Y.V. Lobanov et al., Measurements of cross sections and decay properties of the isotopes of elements 112, 114 and 116 Produced in the Fusion Reactions ^{233,238}U, ^{242}Pu, and ^{248}Cm + ^{48}Ca. Phys. Rev. C **70**, 064609 (2004). https://doi.org/10.1103/PhysRevC.70.064609
56. P.H. Chen, F. Niu, Z.Q. Feng, Production mechanism of proton-rich actinide isotopes in fusion reactions and via multinucleon transfer processes. Phys. Rev. C **102**, 014621 (2020). https://doi.org/10.1103/PhysRevC.102.014621
57. D.C. Zhang, H.G. Cheng, Z.Q. Feng, Hyperon dynamics in heavy-ion collisions near threshold energy. Chin. Phys. Lett. **38**, 092501 (2021). https://doi.org/10.1088/0256-307X/38/9/092501
58. Y.T. Oganessian, F.S. Abdullin, C. Alexander et al., Experimental studies of the ^{249}Bk+^{48}Ca reaction including decay properties and excitation function for isotopes of element 117 and discovery of the new isotope ^{277}Mt. Phys. Rev. C **87**, 054621 (2013). https://doi.org/10.1103/PhysRevC.87.054621
59. V.I. Zagrebaev, W. Greiner, Synthesis of superheavy nuclei: A search for new production reactions. Phys. Rev. C **78**, 034610 (2008). https://doi.org/10.1103/physrevc.78.034610
60. V.I. Zagrebaev, A.V. Karpov, W. Greiner, Possibilities for synthesis of new isotopes of superheavy elements in fusion reactions. Phys. Rev. C **85**, 014608 (2012). https://doi.org/10.1103/PhysRevC.85.014608
61. K. Siwek-Wilczynska, T. Cap, M. Kowal et al., Predictions of the fusion-by-diffusion model for the synthesis cross sections of Z=114-120 elements based on macroscopic-microscopic fission barriers. Phys. Rev. C **86**, 014611 (2012). https://doi.org/10.1103/PhysRevC.86.014611
62. Z.H. Liu, J.D. Bao, Calculation of the evaporation residue cross sections for the synthesis of the superheavy element Z=119 via the ^{50}Ti + ^{249}Bk hot fusion reaction. Phys. Rev. C **84**, 031602(R) (2011). https://doi.org/10.1103/PhysRevC.84.031602
63. K. Siwek-Wilczynska, T. Cap, J. Wilczynski, How can one synthesize the element Z = 120? Int. J. Mod. Phys. E **19**, 500 (2010). https://doi.org/10.1142/S021830131001490X
64. A.K. Nasirov, G. Mandaglio, G. Giardina et al., Effects of the entrance channel and fission barrier in the synthesis of superheavy element Z=120. Phys. Rev. C **84**, 044612 (2011). https://doi.org/10.1103/PhysRevC.84.044612
65. M. Bender, K. Rutz, P.-G. Reinhard et al., Shell structure of superheavy nuclei in self-consistent mean-field models. Phys. Rev. C **60**, 034304 (1999). https://doi.org/10.1103/PhysRevC.60.034304